

Original Article

Promotion of apoptosis and cytochrome c depletion by a low-temperature environment in hindlimb-unloading rats

K. Nagano, H. Hori

Department of Physical Therapy, Faculty of Rehabilitation, Fukui College of Health Sciences, Fukui, Japan

Abstract

Objective: This study aimed to clarify the influence of a low-temperature environment on muscle atrophy and apoptosis. **Methods:** Wistar rats were divided into four groups: two groups of hindlimb-unloading rats maintained in a normal (25°C, HU) or low-temperature (10°C, HU+LT) environment for 3 weeks and two corresponding control groups (CON; normal temperature, CON+LT; low-temperature). **Results:** The soleus muscle wet weight and muscle-to-body mass ratio were lower in the experimental groups than in the control groups. The cross-sectional areas of myofibers in the HU+LT and HU groups were significantly decreased than those in the CON and CON+LT groups. Ubiquitin ladder levels from soleus muscle lysates were significantly increased in the HU+LT group. Caspase-3-activated myofibers were observed only in the HU+LT group. Decreased cytochrome c levels were present in these caspase-3-activated myofibers. Meanwhile, cytochrome c levels were increased significantly in CON+LT rats but unchanged in HU+LT rats. **Conclusion:** Our results suggest that apoptosis caused by hindlimb unloading at low temperatures is associated with a lack of cytochrome c in myofibers. This indicates that long-term hindlimb unloading at low temperatures did not suppress muscle atrophy. We conclude that low-temperature stimulation should not be used as a long-term treatment for preventing disuse atrophy.

Keywords: Disuse, Apoptosis, Low Temperature, Cytochrome c, Hindlimb Unloading

Introduction

Disuse muscle atrophy is caused by prolonged skeletal muscle inactivity and is associated with rapid decreases in muscle mass, muscle fiber size, and strength. The common conditions leading to disuse atrophy include limb immobilization, prolonged bed rest, denervation, chronic pulmonary insufficiency, and a microgravity environment¹.

Muscle atrophy is primarily caused by decreased protein synthesis and increased protein degradation². Recent studies demonstrated that the ubiquitin–proteasome, autophagy–lysosome, and calpain systems as well as oxidative stress and caspase and PI3/Akt/mTOR signaling are largely involved in the

mechanism of muscle atrophy³. Specifically, the aforementioned proteases are overexpressed and activated, whereas PI3/Akt/mTOR signaling is simultaneously inhibited in the sarcoplasm.

Some methods for preventing disuse atrophy have been investigated, such as electrical stimulation, immobilization of the muscle in a relatively lengthened position, and the administration of vitamin E, which is an antioxidant, and inhibitors of calpain or lysosomal proteases^{4–7}. However, their alleviative effects on muscle atrophy were insufficient, and the durations of their protective effect were extremely short.

On the contrary, apoptosis in skeletal muscle results from inactivity or pathological conditions, such as denervation⁸, muscular dystrophy⁹, hindlimb unloading¹⁰, and aging-associated sarcopenia¹¹. Mitochondrial cytochrome c is involved in the initiation of apoptosis. Upon its release into the cytosol, cytochrome c induces the formation of the apoptosome complex by apoptotic protease-activating factor 1 (Apaf1), dATP, and procaspase-9. Apoptosome-bound procaspase-9 is activated, triggering the activation of caspase-3 and leading to the progression of cell death^{11,12}.

Mild therapeutic hypothermia is an induced hypothermia that can maintain body temperature from 34°C to 36°C for 4

The authors have no conflict of interest.

Corresponding author: Katsuhito Nagano, Ph.D., Department of Physical Therapy, Faculty of Rehabilitation, Fukui College of Health Sciences, 56 Egami-cho 13-1, Fukui City, Fukui 910-3190, Japan
E-mail: nagano@xg8.so-net.ne.jp

Edited by: M. Hamrick
Accepted 22 October 2014

days. This technique exerts significant neuroprotection and attenuates secondary cerebral insults after traumatic brain injury¹³. The important mechanism of the neuroprotective effects of moderate hypothermia is the reduction of cerebral energy metabolism and oxygen demand, but the changes induced by mild hypothermia are extremely small¹⁴. Nevertheless, hypothermia similarly inhibits cytosolic cytochrome c release¹⁵ and suppresses the induction of apoptosis in neurons¹⁶. Mild hypothermia decreases the expression of the cysteinyl aspartate-specific proteinase caspase-3 in a caspase-dependent pathway¹⁷. However, the mechanism by which mild hypothermia suppresses apoptosis and the protective effect of decreases in body temperature on other organs remain unclear.

Mammalian hibernators, such as ground squirrels and black bears, exhibit slightly decreased body temperatures during winter to reduce metabolic energy demands^{18,19}. The hibernators display physical inactivity during torpor bouts. Although low mechanical loading during physical inactivity is believed to induce disuse atrophy in skeletal muscle, hibernators experience relatively low levels of muscle atrophy compared with the findings in experimental models of disuse atrophy, such as limb immobilization and hindlimb unloading^{20,21}. Genes involved in apoptosis tend to be downregulated in the bones of black bears during hibernation²². It is reported that caspase-3-specific activity in the intestinal mucosa is repressed in ground squirrels during hibernation²³.

However, the effect of hibernation or low temperatures on the expression of apoptosis-related genes in skeletal muscle is poorly understood. Stimulation of hibernation for preventive effects of muscle atrophy and that of mild therapeutic hypothermia for neuroprotective effects is common. Low-temperature environment may be a common stimulation. In hibernating animals and rat stroke models, the important effect by low-temperature environment is not that the body core temperature decreases but that the body could be exposed to low-temperature stimulation^{24,25}.

In Wistar rats, which do not hibernate, we clarified that the occurrence of apoptosis is increased in a low-temperature environment compared with the findings in a normal environment, indicating that long-term low-temperature maintenance cannot suppress muscle atrophy in the absence of hindlimb loading. In other words, we observed that low-temperature environment in hindlimb-unloading rats accelerates the occurrence of apoptosis over long durations²⁶.

However, the relationship between the expression of apoptosis-related and energy metabolism-related genes in hindlimb-unloading animals in a low-temperature environment is unclear. To clarify the reasons for the observed expression-enhancing action of muscle apoptosis, we investigated the changes in the expression levels of mitochondrial enzymes in hindlimb-unloading rats exposed to low temperatures.

Materials and methods

Study groups and tissue preparation

This investigation was conducted in accordance with the ethical guidelines for the experimental treatment of animals of

the School of Medicine, Hiroshima University.

Nine-week-old male Wistar rats weighing 275±9 g were housed in individual cages and randomly assigned to four groups (5 rats/group). Rats underwent hindlimb unloading at 10°C (HU+LT) or 25°C (HU) for 3 weeks, whereas the other two (control) groups were not subjected to hindlimb unloading and were maintained at 10°C (CON+LT) or 25°C (CON). Hindlimb unloading was achieved by elevating the hindlimbs and preventing them from touching a supporting surface. The forelimbs maintained contact with a grid floor, which allowed the animals a full range of motion. Food and water were provided *ad libitum*.

At the end of the experimental period, rats were anesthetized with an intraperitoneal injection of 50 mg/kg pentobarbital sodium (Abbott Laboratories, North Chicago, IL, USA), weighed, and sacrificed by laparotomy followed by transection of the abdominal aorta. The soleus muscles were immediately excised and cut transversely into two segments. Each segment was individually mounted on cork using optimum cutting temperature compound (Sakura Finetek USA, Torrance, CA, USA), and then the blocks were rapidly snap frozen in isopentane cooled in liquid nitrogen and stored at -80°C.

Fluorescence immunohistochemistry

To determine the number of active caspase-3-positive myofibers per transverse section and observe the immunolabeling of apoptotic factors, 8-µm thick serial transverse cryosections were cut from tissue blocks using a cryostat microtome at -25°C and mounted on silane-coated glass slides (Matsunami, Osaka, Japan). After air-drying for 60 min at room temperature, the serial cryosections were fixed in cold acetone at 4°C and then air-dried for 60 min.

The serial transverse cryosections were immersed three times, for 5 min each, in 0.01 M phosphate-buffered saline (PBS, pH 7.4), and then non-specific immunoglobulin (Ig) binding sites in the tissue were blocked by incubation for at least 60 min in 1% normal bovine serum albumin (BSA, Sigma-Aldrich, St. Louis, MO, USA) in PBS. Serial sections were incubated overnight at 4°C in the presence of one of the primary antibodies directed against caspase-3 and cytochrome c diluted in 1% BSA in PBS. The sections were then incubated for 3 h with Alexa 546-conjugated anti-rabbit IgG (Molecular Probes, Eugene, OR, USA), each diluted 1:200, and mounted in a mixture of PBS and glycerol (1:3) containing 0.1% *p*-phenylenediamine to prevent fading of the immunofluorescence.

All dilutions and thorough washes between steps were performed using PBS at room temperature unless otherwise specified. Incubations with primary and secondary antisera were performed in a darkened, humidified chamber.

The sections were examined using a confocal laser-scanning microscope equipped with argon and helium/neon lasers (LSM-510; Carl Zeiss, Jena, Germany).

Protein isolation procedures

Whole muscle lysates were isolated by homogenizing freshly excised muscle in 10 vol of lysis buffer containing 50

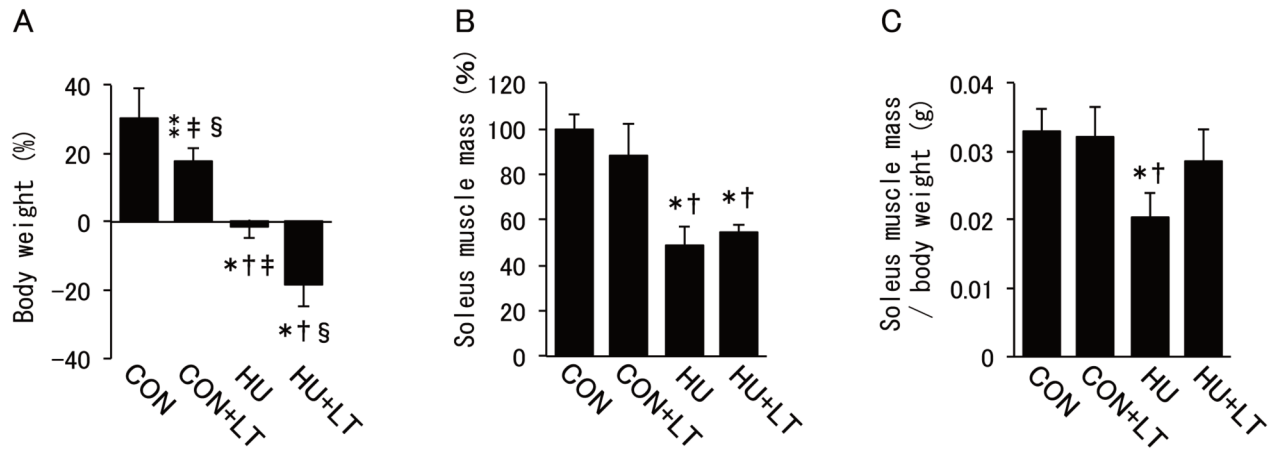


Figure 1. Difference in body weight before and after the 3-week period of low-temperature environment. A: % body weight (the body weight changes are expressed as an increase or decrease from the body weight before the experiment), B: % soleus muscle mass (muscle mass/CON), C: ratio of muscle mass (muscle mass/body weight). Values are presented as means \pm SD. CON rats were hindlimb-loaded in a normal temperature environment at 25°C. CON+LT rats were hindlimb-loaded in a low-temperature environment at 10°C. HU+LT rats were hindlimb-unloaded in a low-temperature environment at 10°C. HU rats were hindlimb-unloaded in a normal temperature environment at 25°C. * P <0.01 vs. CON, * P <0.05 vs. CON, † P <0.05 vs. CON+LT, ‡ P <0.05 vs. HU+LT, § P <0.05 vs. HU.

mM Tris-HCl, pH 7.4, 150 mM NaCl, 1 mM ethylenediaminetetraacetic acid (Nacalai Tesque, Kyoto, Japan), 1 mM ethylene glycol-bis[β -aminoethyl ether]-N,N,N',N'-tetraacetic acid (Sigma), 10 mg/ml aprotinin (Sigma), 10 mg/ml leupeptin (Sigma), 1 mg/ml pepstatin (Sigma), and 1 mM phenylmethylsulfonyl fluoride (Sigma) on ice. Homogenates were centrifuged at 10,000 \times g for 10 min at 4°C to remove nuclear fragments and tissue debris without precipitating the plasma membrane, and the supernatants were used for western blotting analyses. The protein concentrations were determined by the Bradford method²⁷ using Ig as the standard (Bio-Rad, Hercules, CA, USA). All proteins were denatured by boiling at 90°C for 3 min in 1:1 (vol/vol) sample buffer containing 2% sodium dodecyl sulfate (SDS) (Sigma), 50 mM Tris-HCl (pH 6.8), 10% 2-mercaptoethanol, 10% glycerol, and 0.1% bromophenol blue (Nacalai Tesque). Denatured proteins were electrophoresed in 10% SDS-polyacrylamide gels and transferred to nitrocellulose membranes (Bio-Rad). The membranes were blocked overnight with blocking buffer [25 mM Tris-buffered saline (TBS)] containing 5% skimmed milk) at 4°C and incubated at room temperature for 3 h in a primary antibody diluted in blocking buffer. The primary antibodies were directed against cytochrome c, ubiquitin, and actin.

The membranes were washed three times with 0.1% Tween-TBS, probed with a secondary biotinylated anti-mouse or anti-rabbit IgG, as described previously, diluted 1:2000 in blocking buffer for 2 h, and then washed three times. The membranes were then incubated for 1 h with ABC reagent (Vector Laboratories, Burlingame, CA, USA), prepared according to manufacturer's instructions, and labeling was detected with 0.01% DAB and 0.05% H₂O₂ in 50 mM Tris-HCl buffer (pH 7.6) for 15 min, as described previously. The reaction was stopped by

washing the sections in running water. Quantification of the signal was performed by densitometric analysis using NIH Image Ver. 1.62 software (National Institutes of Health, Bethesda, MD, USA).

Quantitative analysis

The cross-sectional areas of tissue sections of each sample were examined using light microscopy, and the numbers of caspase-3-positive myofibers were counted on digitized images of the fluorescence microscopy. Photographs of cross-sections of whole muscles were taken using a light microscope, digitized with a CCD camera (Eclipse E600; Nikon, Tokyo, Japan) linked to a computer equipped with a frame grabber, and subsequently processed to calculate the cross-sectional areas of an average of 100 fibers of each type per muscle using Image Ver. 1.62 software. Fiber types were classified by immunolabeling for the slow and fast myosin heavy chains.

All values are expressed as the mean \pm SE. The results obtained from all experiments were analyzed by one-way analysis of variance followed by Tukey's honestly significant difference post hoc multiple-comparison test with the significance level set at P <0.05.

Results

It was visually observed that the HU+LT group became less active earlier than the other groups after entering the low-temperature environment. The CON+LT group was also observed to become less active than the CON group, excluding the feeding behavior. Observations after the experiment revealed no

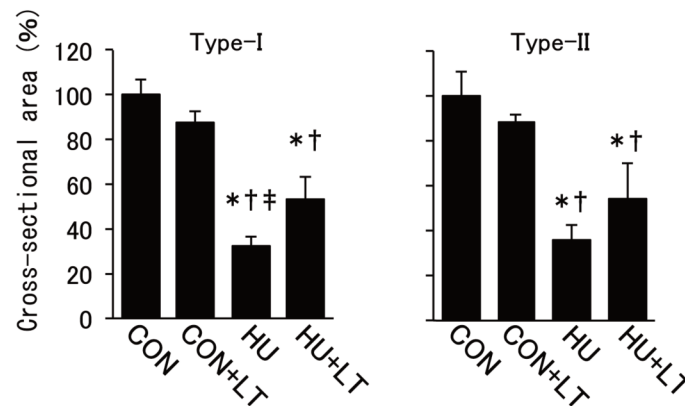


Figure 2. Comparison of the mean cross-sectional areas of type I and II fibers in soleus muscle. Values are presented as means \pm SD. * $P < 0.01$ vs. CON, † $P < 0.01$ vs. CON+LT, ‡ $P < 0.01$ vs. HU+LT.

morphological abnormalities in the lower limbs of the CON+LT, HU+LT, and HU animals.

Body weight

The body weights before and after experiment were measured and compared among the groups. The percentage changes of body weight were $30.5 \pm 8.8\%$, $17.7 \pm 3.6\%$, $-18.2 \pm 6.5\%$, and $-1.5 \pm 3.4\%$ in the CON, CON+LT, HU+LT, and HU groups, respectively. Significant differences in body weight were observed among the groups (Figure 1A).

Muscle wet weight

The wet weight of the soleus muscle after the experiment was measured and compared among the groups. The muscle wet weight was lower in the CON+LT ($11.5 \pm 13.6\%$), HU+LT ($45.8 \pm 3.9\%$), and HU groups ($51.4 \pm 8.2\%$) than in the CON group. In addition, the muscle wet weights of the HU+LT and HU groups were significantly decreased compared with those of the CON and CON+LT groups. However, the slight difference between the CON and CON+LT groups was not statistically significant (Figure 1B).

Muscle-to-body mass ratio

The muscle-to-body mass ratio was lower in the CON+LT ($2.2 \pm 12.9\%$), HU+LT ($12.9 \pm 13.9\%$), and HU groups ($38.2 \pm 10.9\%$) than in the CON group. Furthermore, the muscle-to-body mass ratio of the HU group was significantly decreased compared with those of the CON, CON+LT, and HU+LT groups. No differences were observed between the CON and HU+LT groups (Figure 1C).

Cross-sectional area of muscle fibers

The cross-sectional area of type I muscle fibers was decreased by $12.1 \pm 5.0\%$, $46.5 \pm 9.9\%$, and $67.9 \pm 4.8\%$ in the CON+LT, HU+LT, and HU groups, respectively, compared

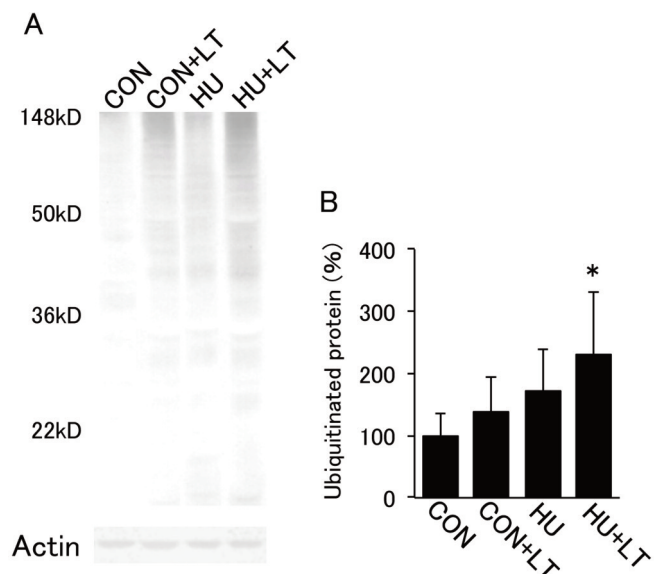


Figure 3. Broad band of immunoreactivity that was composed of ubiquitinated muscle proteins (A). Whole muscle lysates were visualized by immunoblot analysis, and data from each experimental group were quantified (B). Values are presented as means \pm SD. * $P < 0.05$ vs. CON.

with that in the CON group. The cross-sectional area of type I muscle fibers in HU+LT rats was significantly decreased compared with that in CON and CON+LT rats, and the cross-sectional area of these fibers in HU rats was significantly lower than that in the other groups. The slight difference in cross-sectional area between CON and CON+LT rats was not statistically significant (Figure 2).

The cross-sectional area of type II muscle fibers was decreased by $11.9 \pm 3.6\%$, $46.0 \pm 15.8\%$, and $64.1 \pm 6.7\%$, in CON+LT, HU+LT, and HU rats, respectively, compared with

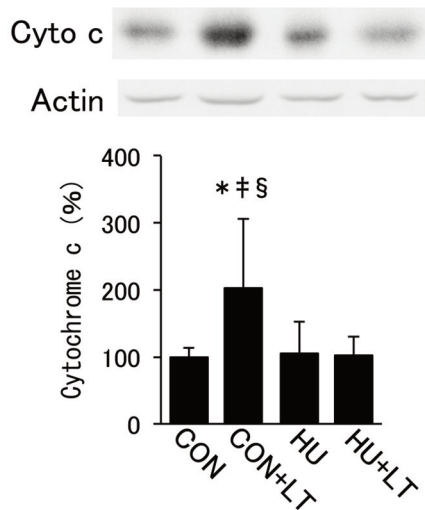


Figure 4. Cytochrome c protein content in soleus muscle. Western blot illustrating the increase in cytochrome c protein expression in CON+LT rats. Values are presented as means \pm SD. ^{*}P<0.05 vs. CON, [†]P<0.05 vs. HU+LT, [§]P<0.05 vs. HU.

that in CON rats. In addition, the cross-sectional area of these fibers was significantly lower in the HU+LT and HU groups than in the CON and CON+LT groups. The difference in this variable between CON and CON+LT rats was not statistically significant (Figure 2).

Western blot analysis of cytochrome c and ubiquitinated proteins

Ubiquitin-tagged proteins are degraded via the ubiquitin–proteasome pathway. To compare the progress of ubiquitination, whole muscle lysates were analyzed by western blotting with anti-ubiquitin.

Broad bands in a ladder-like electrophoretic pattern expanding downward from the top of the lane were strongly present in HU+LT lysates, but the bands were hardly detectable in CON lysates. Compared with CON lysates, the total levels of ladder bands were increased by 2.3 fold in HU+LT lysates, whereas the levels were not significantly different between CON+LT and HU lysates (Figure 3).

Cytochrome c serves as an initiator in the mitochondrial apoptosis pathway and participates in the regulation of energy metabolism in skeletal muscle. The relative levels of cytochrome c in the soleus muscles in the four groups were analyzed by western blotting. Compared with the findings in the CON group, cytochrome c levels were increased by 2.3 ± 0.9 fold in the CON+LT group, versus 1.0 ± 0.3 and 1.3 ± 0.6 fold in the HU+LT and HU groups, respectively (Figure 4).

Quantitative analysis of active caspase-3 in whole muscle

Cytochrome c immunolabeling was evident in the subsarcolemmal regions of intact myofibers and visible as small, weakly labeled dots in sarcoplasmic masses in HU+LT rats,

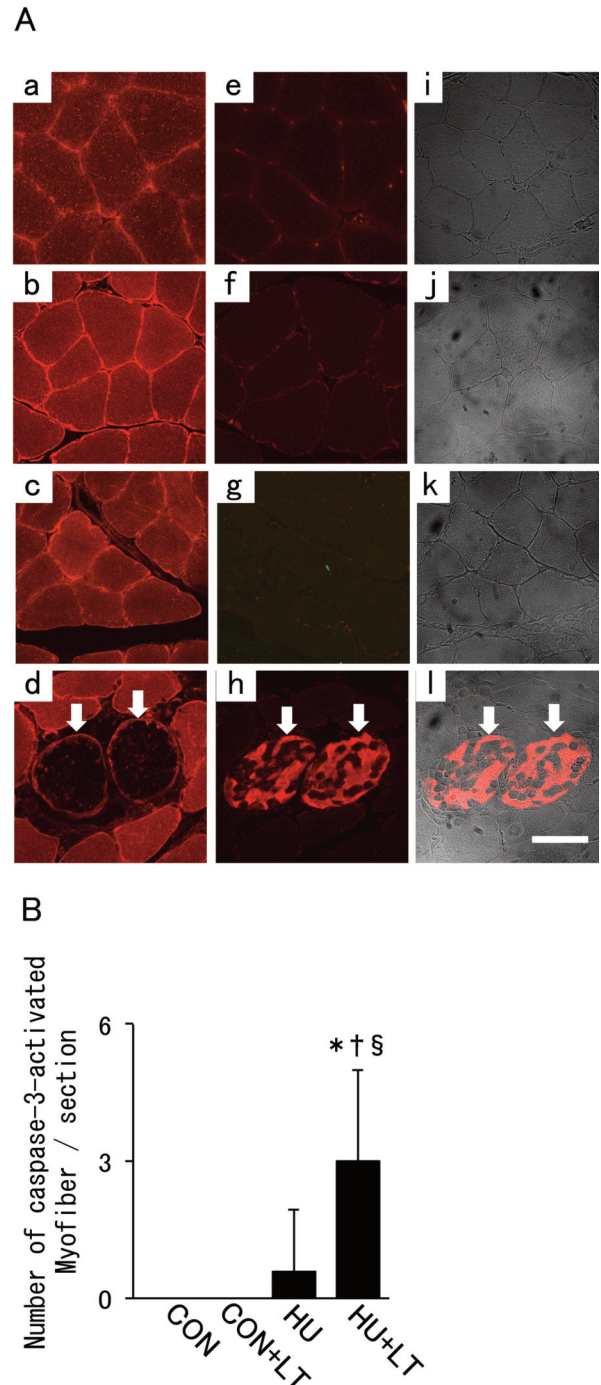


Figure 5. Morphological aspects and immunopositivity of cytochrome c in active caspase-3-positive myofibers (A) and mean number of active caspase-3-positive myofibers in a muscle cross-section (B). Transverse serial sections of the soleus muscle labeled with anti-cytochrome c (a-d) or anti-active caspase-3 (e-l) antibody are shown. Active caspase-3-positive myofibers were observed in HU+LT rats (h and l) but not in CON (e and i), CON+LT (f and j), and HU rats (g and k). Cytochrome c immunolabeling was evident in the subsarcolemmal regions of intact myofibers. This immunolabeling was markedly absent in active caspase-3-positive myofibers (d). Arrows denote the same myofibers as the caspase-3-activated myofibers in the serial sections. Scale bars: 50 μ m. Values are presented as means \pm SD. ^{*}P<0.01 vs. CON, [†]P<0.01 vs. CON+LT, [§]P<0.01 vs. HU.

whereas this immunolabeling was markedly absent in active caspase-3-positive myofibers (Figure 5A).

The mean numbers of active caspase-3-positive myofibers per section were 3.0 ± 2.0 and 0.6 ± 1.3 in HU+LT and HU rats, respectively, whereas active caspase-3 immunolabeling was not detected in CON and CON+LT rats by confocal microscopy. The numbers of active caspase-3-positive myofibers were significantly increased in HU+LT rats compared with that in CON and CON+LT rats, and the small number of positive myofibers in HU rats displayed no significant difference (Figure 5B).

Discussion

Hibernators such as ground squirrels and black bears display maintenance of muscle mass against disuse atrophy despite prolonged periods of inactivity^{28,29}. A previous study revealed that the protein turnover rate in black bears increases during hibernation compared with that before hibernation or dormancy³⁰. Another study illustrated that protein synthesis and breakdown are suppressed in black bears in winter compared to summer³¹. In any case, the important mechanism by which atrophy is prevented would be that the rate of protein breakdown typically does not exceed that of protein synthesis.

In contrast, the results of this study demonstrated that hindlimb-unloading rats develop muscle atrophy in both normal and low-temperature environments judging from the myofiber size and total amount of ubiquitin ladder protein. In association with the changes in myofiber size, previous studies of hindlimb-unloading rats revealed that muscle atrophy was primarily the result of decreased intracellular protein synthesis and increased intracellular protein degradation³².

The ubiquitin proteasome system is one of the major pathways involved in regulating muscle protein degradation, playing a central role in controlling muscle mass and fiber size^{33,34}. In this system, proteins that are degraded are first marked with a polyubiquitin degradation signal. Ubiquitination is performed by ubiquitin-activating enzyme (E1), and E1 and ubiquitin-conjugating proteins (E2) prepare ubiquitin for conjugation. Ubiquitin-protein ligase (E3) recognizes a specific protein substrate. Polyubiquitinated protein substrates are then specifically recognized and finally degraded by the 26S proteasome³⁵. Our results indicated that intracellular protein turnover rates cannot be maintained normally even in a low-temperature environment because low temperatures do not inhibit activation of the ubiquitin-proteasome system. On the contrary, low-temperature stimulation accelerates protein ubiquitination in unloading rats. Thus, it is evident that low-temperature stimulation does not prevent the reduction of the myofiber cross-sectional area without muscle tension in non-hibernating animals.

In this study, the number of apoptotic myofibers was elevated in hindlimb-unloading rats exposed to the low-temperature environment compared with the findings in the normal-temperature environment. The caspase-3-activated myofibers were characterized by extremely low immunofluorescence or the absence of cytochrome c relative to the non-

apoptotic myofibers. In general, the mitochondrial-dependent apoptosis pathway induces caspase-3 activation. The pathway is initiated by the release of cytochrome c from the mitochondria into the cytoplasm, where it then forms an apoptosome and promotes the activation of caspase-9 and caspase-3. Caspase-3 plays a key role in apoptosis in various tissues and is an effector caspase involved in the execution of apoptosis. In a previous study using rotenone, which induces apoptosis by activating a mitochondria-dependent caspase pathway, rotenone-treated rat pituitary cells displayed colocalization of cytochrome c and Apaf-1 during the activation of apoptosis. Immunostaining revealed that cytochrome c and Apaf-1 formed an apoptosome in the treated cells. These expression and localization data were confirmed visually by confocal microscopy³⁶. The key points are that part of the apoptosome component was positive for cytochrome c immunostaining and that cytochrome c immunostaining was positive in the early stage of the mitochondrial-dependent apoptosis pathway. Morphologically, the caspase-3-activated myofibers observed in our study differed from those observed in rotenone-treated pituitary cells in the early stage of apoptosis³⁶.

It has been reported that HeLa cells induce apoptosis upon exposure to UVB irradiation. On immunostaining, these apoptotic cells exhibit overexpression and diffusion of cytochrome c, caspase activity, and chromatin condensation³⁷. The immunohistochemical features of apoptotic myofibers observed in our study differed fundamentally from those of UVB-treated apoptosis in the lack of cytochrome c expression.

The forkhead box O3 (FoxO3) transcription factor has been reported to mediate protein degradation in skeletal muscle by activating the ubiquitin-proteasome pathway and the autophagy-lysosome pathway³⁸. The activity of ubiquitin-proteasomes, mainly two muscle-specific ubiquitin ligases (atrogin-1/MAFbx and MuRF1), causes marked muscle atrophy³⁹. On the other hand, Atg7 knockout mice, which are deficient in a gene essential for autophagy, show accumulation of dysfunctional mitochondria and formation of aberrant concentric membranous structures. As a result, the inhibition of autophagy is estimated to contribute to caspase activation and apoptosis by affecting the permeability transition pore opening⁴⁰. Conversely, Akt (protein kinase B)/mTOR (the mammalian target of rapamycin) signaling can result in enhanced protein synthesis and skeletal muscle hypertrophy by phosphorylating FoxO proteins⁴¹. Hence, the muscle atrophy and apoptosis that was observed in this study may have been mutually associated with the crosstalk and imbalances of the ubiquitin-proteasomal pathway, autophagy-lysosome pathway, and Akt/mTOR pathway.

The reason for these findings may be that the progressive stage of caspase-3-activated myofibers reflects the terminal stage opposed to the early stage of apoptosis. Another possibility is that mitochondria cytochrome c leaked from the sarcolemma to the extracellular environment in this stage. Moreover, it is also speculated that cytochrome c in caspase-3-activated myofibers was exhausted or that its generation was limited.

Although caspase-3 knockout mice exhibit significantly at-

tenuated muscle mass and decreased immobilization-induced apoptotic myonuclei, the upregulation of the muscle-specific E3 ligases (i.e., atrogin-1 and MuRF1) during immobilization does not require caspase-3 activation⁴². In our observation, ubiquitination progressed in HU+LT rats, but few caspase-3-activated myofibers were present in the whole muscle cross-section. Our results also suggested that ubiquitination in muscle atrophy does not require caspase-3 activation.

The gastrocnemius muscle of frogs, when exposed to cold temperature, display increased citrate synthase and cytochrome oxidase activities⁴³, similar to the findings in the red muscle of fish⁴⁴. The skeletal muscle mitochondria of young pigs raised in a low-temperature environment exhibit increased mitochondrial protein levels and cytochrome c concentrations⁴⁵. In previous studies, a low-temperature environment tended to increase mitochondrial enzyme activities in skeletal muscle⁴⁶. In this study, CON+LT rats displayed increased cytochrome c production in response to exposure to low temperatures, whereas HU+LT rats did not exhibit increased cytochrome c production. Muscle atrophy resulting from denervation occurs in conjunction with reductions in mitochondrial content and function⁴⁷. There is also a decline in mitochondrial content during muscle atrophy, as observed in this study. This decrease may be suggestive of a reduced capacity for mitochondria-dependent apoptosis.

Cold exposure is supposed to decrease muscle proteolysis and attenuate muscle atrophy in skeletal muscle protein metabolism. However, our results showed that muscle atrophy was not inhibited, which implies that there were no such effects of long-term low temperatures. Short-term cold exposure has been reported to increase proteolysis of muscle⁴⁸. In contrast, myoblasts acutely exposed to cold temperatures have decreased apoptosis, collapsed membrane potentials, and increased cell viability⁴⁹. Previously, we showed that a low-temperature environment for 1 week prevented slow-to-fast skeletal muscle fiber conversion⁵⁰. These findings may indicate that the initial effect of low temperature maintains energy metabolism in muscle fibers and not protein metabolism.

It has been suggested that hindlimb unloading-induced apoptosis at low temperatures is caused by a lack of ATP production because of reduced cytochrome c levels in myofibers. Our results indicate that long-term hindlimb unloading did not suppress muscle atrophy in a low-temperature environment. Therefore, we concluded that long-term unloading conditions should not be permitted in low temperatures.

References

1. Zhang P, Chen X, Fan M. Signaling mechanisms involved in disuse muscle atrophy. *Med Hypotheses* 2007;69:310-21.
2. Gamrin L, Berg HE, Essén P, Tesch PA, man E, Garlick PJ, McNurlan MA, Wernerman J. The effect of unloading on protein synthesis in human skeletal muscle. *Acta Physiol Scand* 1998;163:369-77.
3. Dupont E, Cieniewski-Bernard C, Bastide B, Stevens L. Electrostimulation during hindlimb unloading modulates PI3K-AKT downstream targets without preventing soleus atrophy and restores slow phenotype through ERK. *Am J Physiol Regul Integr Comp Physiol* 2011;300:R408-17.
4. Dirks ML, Wall BT, Snijders T, Ottenbros CL, Verdijk LB, van Loon LJ. Neuromuscular electrical stimulation prevents muscle disuse atrophy during leg immobilization in humans. *Acta Physiol (Oxf)* 2014;210:628-41.
5. Servais S, Letexier D, Favier R, Duchamp C, Desplanches D. Prevention of unloading-induced atrophy by vitamin E supplementation: links between oxidative stress and soleus muscle proteolysis? *Free Radic Biol Med* 2007;42:627-35.
6. Fareed MU, Evenson AR, Wei W, Menconi M, Poylin V, Petkova V, Pignol B, Hasselgren PO. Treatment of rats with calpain inhibitors prevents sepsis-induced muscle proteolysis independent of atrogin-1/MAFbx and MuRF1 expression. *Am J Physiol Regul Integr Comp Physiol* 2006;290:R1589-97.
7. Libby P, Goldberg AL. Leupeptin, a protease inhibitor, decreases protein degradation in normal and diseased muscles. *Science* 1978;199:534-6.
8. Adhihetty PJ, O'Leary MF, Chabi B, Wicks KL, Hood DA. Effect of denervation on mitochondrially mediated apoptosis in skeletal muscle. *J Appl Physiol* 2007;102:1143-51.
9. Sandri M, El Meslemani AH, Sandri C, Schjerling P, Vissing K, Andersen JL, Rossini K, Carraro U, Angelini C. Caspase 3 expression correlates with skeletal muscle apoptosis in Duchenne and facioscapulo human muscular dystrophy. A potential target for pharmacological treatment? *J Neuropathol Exp Neurol* 2001;60:302-12.
10. Siu PM, Pistilli EE, Butler DC, Alway SE. Aging influences cellular and molecular responses of apoptosis to skeletal muscle unloading. *Am J Physiol Cell Physiol* 2005;288:C338-49.
11. Marzetti E, Wohlgemuth SE, Lees HA, Chung HY, Giovannini S, Leeuwenburgh C. Age-related activation of mitochondrial caspase-independent apoptotic signaling in rat gastrocnemius muscle. *Mech Ageing Dev* 2008;129:542-9.
12. Siu PM, Alway SE. Mitochondria-associated apoptotic signalling in denervated rat skeletal muscle. *J Physiol* 2005;565:309-23.
13. Campbell K, Knuckey NW, Brookes LM, Meloni BP. Efficacy of mild hypothermia (35°C) and moderate hypothermia (33°C) with and without magnesium when administered 30min post-reperfusion after 90min of middle cerebral artery occlusion in Spontaneously Hypertensive rats. *Brain Res* 2013;1502:47-54.
14. Mori K, Maeda M, Miyazaki M, Iwase H. Effects of mild (33 degrees C) and moderate (29 degrees C) hypothermia on cerebral blood flow and metabolism, lactate, and extracellular glutamate in experimental head injury. *Neurol Res* 1998;20:719-26.
15. Zhao H, Wang JQ, Shimohata T, Sun G, Yenari MA,

- Sapolsky RM, Steinberg GK. Conditions of protection by hypothermia and effects on apoptotic pathways in a rat model of permanent middle cerebral artery occlusion. *J Neurosurg* 2007;107:636-41.
16. Van Hemelrijck A, Vermijlen D, Hachimi-Idrissi S, Sarre S, Ebinger G, Michotte Y. Effect of resuscitative mild hypothermia on glutamate and dopamine release, apoptosis and ischaemic brain damage in the endothelin-1 rat model for focal cerebral ischaemia. *J Neurochem* 2003;87:66-75.
 17. Zgavc T, De Geyter D, Ceulemans AG, Stoop W, Hachimi-Idrissi S, Michotte Y, Sarre S, Kooijman R. Mild hypothermia reduces activated caspase-3 up to 1 week after a focal cerebral ischemia induced by endothelin-1 in rats. *Brain Res* 2013;1501:81-8.
 18. Tøien Ø, Blake J, Edgar DM, Grahn DA, Heller HC, Barnes BM. Hibernation in black bears: independence of metabolic suppression from body temperature. *Science* 2011;331:906-9.
 19. Henry PG, Russeth KP, Tkac I, Drewes LR, Andrews MT, Gruetter R. Brain energy metabolism and neurotransmission at near-freezing temperatures: *in vivo* (1)H MRS study of a hibernating mammal. *J Neurochem* 2007;101:1505-15.
 20. Steffen JM, Koebel DA, Musacchia XJ, Milsom WK. Morphometric and metabolic indices of disuse in muscles of hibernating ground squirrels. *Comp Biochem Physiol B* 1991;99:815-9.
 21. James RS, Staples JF, Brown JC, Tessier SN, Storey KB. The effects of hibernation on the contractile and biochemical properties of skeletal muscles in the thirteen-lined ground squirrel, *Ictidomys tridecemlineatus*. *J Exp Biol* 2013;216:2587-94.
 22. Fedorov VB, Goropashnaya AV, Tøien Ø, Stewart NC, Chang C, Wang H, Yan J, Showe LC, Showe MK, Donahue SW, Barnes BM. Preservation of bone mass and structure in hibernating black bears (*Ursus americanus*) through elevated expression of anabolic genes. *Funct Integr Genomics* 2012;12:357-65.
 23. Fleck CC, Carey HV. Modulation of apoptotic pathways in intestinal mucosa during hibernation. *Am J Physiol Regul Integr Comp Physiol* 2005;289:R586-95.
 24. Horwitz BA, Chau SM, Hamilton JS, Song C, Gorgone J, Saenz M, Horowitz JM, Chen CY. Temporal relationships of blood pressure, heart rate, baroreflex function, and body temperature change over a hibernation bout in Syrian hamsters. *Am J Physiol Regul Integr Comp Physiol* 2013;305:R759-68.
 25. Yager JY, Asselin J. Effect of mild hypothermia on cerebral energy metabolism during the evolution of hypoxic-ischemic brain damage in the immature rat. *Stroke* 1996;27:919-25.
 26. Nagano K, Suzaki E, Nagano Y, Kataoka K, Ozawa K. The activation of apoptosis factor in hindlimb unloading-induced muscle atrophy under normal and low-temperature environmental conditions. *Acta Histochem* 2008;110:505-18.
 27. Bradford MM. A rapid and sensitive method for the quantitation of microgram quantities of protein utilizing the principle of protein-dye binding. *Anal Biochem* 1976;72:248-54.
 28. Xu R, Andres-Mateos E, Mejias R, MacDonald EM, Leinwand LA, Merriman DK, Fink RH, Cohn RD. Hibernating squirrel muscle activates the endurance exercise pathway despite prolonged immobilization. *Exp Neurol* 2013;247:392-401.
 29. Nowell MM, Choi H, Rourke BC. Muscle plasticity in hibernating ground squirrels (*Spermophilus lateralis*) is induced by seasonal, but not low-temperature, mechanisms. *J Comp Physiol B* 2011;181:147-64.
 30. Lundberg DA, Nelson RA, Wahner HW, Jones JD. Protein metabolism in the black bear before and during hibernation. *Mayo Clin Proc* 1976;51:716-22.
 31. Lohuis TD, Harlow HJ, Beck TD. Hibernating black bears (*Ursus americanus*) experience skeletal muscle protein balance during winter anorexia. *Comp Biochem Physiol B Biochem Mol Biol* 2007;147:20-8.
 32. Goldspink DF. The influence of immobilization and stretch on protein turnover of rat skeletal muscle. *J Physiol* 1977;264:267-82.
 33. Taillandier D, Aurousseau E, Meynial-Denis D, Bechet D, Ferrara M, Cottin P, Ducastaing A, Bigard X, Guezennec CY, Schmid HP, Attaix D. Coordinate activation of lysosomal, Ca²⁺-activated and ATP-ubiquitin-dependent proteinases in the unweighted rat soleus muscle. *Biochem J* 1996;316:65-72.
 34. Beehler BC, Sleph PG, Benmassaoud L, Grover GJ. Reduction of skeletal muscle atrophy by a proteasome inhibitor in a rat model of denervation. *Exp Biol Med* (Maywood) 2006;231:335-41.
 35. Stewart HL, Alfred LG, William EM. Protein Degradation by the Ubiquitin-Proteasome Pathway in Normal and Disease States. *JASN* 2006;1807-19.
 36. Potokar M, Kreft M, Chowdhury HH, Vardjan N, Zorec R. Subcellular localization of Apaf-1 in apoptotic rat pituitary cells. *Am J Physiol Cell Physiol* 2006;290:C672-7.
 37. Bossy-Wetzel E, Newmeyer DD, Green DR. Mitochondrial cytochrome c release in apoptosis occurs upstream of DEVD-specific caspase activation and independently of mitochondrial transmembrane depolarization. *EMBO J* 1998;17:37-49.
 38. Mammucari C, Milan G, Romanello V, Masiero E, Rudolf R, Del Piccolo P, Burden SJ, Di Lisi R, Sandri C, Zhao J, Goldberg AL, Schiaffino S, Sandri M. FoxO3 controls autophagy in skeletal muscle *in vivo*. *Cell Metab* 2007;6:458-71.
 39. Gomes MD, Lecker SH, Jagoe RT, Navon A, Goldberg AL. Atrogin-1, a muscle-specific F-box protein highly expressed during muscle atrophy. *Proc Natl Acad Sci U S A* 2001;98:14440-5.
 40. Masiero E, Agatea L, Mammucari C, Blaauw B, Loro E, Komatsu M, Metzger D, Reggiani C, Schiaffino S, Sandri M. Autophagy is required to maintain muscle mass. *Cell*

- Metab 2009;10:507-15.
41. Norrby M, Evertsson K, Fjällström AK, Svensson A, Tågerud S. Akt (protein kinase B) isoform phosphorylation and signaling downstream of mTOR (mammalian target of rapamycin) in denervated atrophic and hypertrophic mouse skeletal muscle. *J Mol Signal* 2012;7:7.
 42. Zhu S, Nagashima M, Khan MA, Yasuhara S, Kaneki M, Martyn JA. Lack of caspase-3 attenuates immobilization-induced muscle atrophy and loss of tension generation along with mitigation of apoptosis and inflammation. *Muscle Nerve* 2013;47:711-21.
 43. Ohira M, Ohira Y. Effects of exposure to cold on metabolic characteristics in gastrocnemius muscle of frog (*Rana pipiens*). *J Physiol* 1988;395:589-95.
 44. Johnston IA, Sidell BD, Driedzic WR. Force-velocity characteristics and metabolism of carp muscle fibres following temperature acclimation. *J Exp Biol* 1985;119:239-49.
 45. Cheah KS, Dauncey MJ, Cheah AM, Ingram DL. Influence of environmental temperature and energy intake on porcine skeletal muscle mitochondria. *Comp Biochem Physiol B* 1985;82:287-92.
 46. Battersby BJ, Moyes CD. Influence of acclimation temperature on mitochondrial DNA, RNA, and enzymes in skeletal muscle. *Am J Physiol* 1998;275:R905-12.
 47. Wicks KL, Hood DA. Mitochondrial adaptations in denervated muscle: relationship to muscle performance. *Am J Physiol Cell Physiol* 1991;260:C841-50.
 48. Ferry AL, Vanderklish PW, Dupont-Versteegden EE. Enhanced survival of skeletal muscle myoblasts in response to overexpression of cold shock protein RBM3. *Am J Physiol Cell Physiol* 2011;301:C392-402.
 49. Manfredi LH, Zanon NM, Garófalo MA, Navegantes LC, Kettelhut IC. Effect of short-term cold exposure on skeletal muscle protein breakdown in rats. *J Appl Physiol* 2013;115:1496-505.
 50. Nagano K, Suzakii E, Nagano Y, Kataoka K, Ozawai K. A Low Temperature Environment Delays the Changes in Muscle Fiber Type Composition Induced by Unloading. *Acta Histochem Clytochem* 2005;38:305-12.